Rheo-SANS: Gap-Resolved SANS of Shear-Induced Alignment of Wormlike Micelles

M. Liberatore, F. Nettesheim and N. J. Wagner
University of Delaware
Newark, DE 19716

L. Porcar
NIST Center for Neutron Research
National Institute of Standards and Technology
Gaithersburg, MD 20899-8562
and
University of Maryland
College Park, MD 20742

Wormlike micellar solutions formed by self-assembled surfactants exhibit rheological properties such as shear thinning and suppression of turbulent flow that are related to the flow-induced changes in their structural conformations or orientations. These flow properties are of relevance in such applications as thickeners, drag reducers and flow improvers in the food and cosmetics industries.

In this highlight we report measurements of the microstructure of a shear-induced phase separating (SIPS) wormlike micellar solution by performing small angle neutron scattering (SANS) measurement using a novel shear cell capable of gap-resolved measurement in the **1-2** (velocity velocity-gradient) plane. Quantitative results show evidence for shear-induced microphase separation accompanied by shear banding. The results suggest that both concentration fluctuations and gradients in segmental alignment occur during SIPS.

The nonlinear rheological behavior of complex fluids includes rich phenomena such as shear-induced phase separation (SIPS). Although many polymeric and self-assembled systems show a wide variety of related phenomena, self-assembled solutions of surfactants forming wormlike micelles [1] have proven to be especially robust in exhibiting clear signatures of SIPS and as such, are of significant scientific interest [2–4]. A rheological signature of SIPS in wormlike micelles is a stress plateau. Models suggest this corresponds to a multi-phase flow regime composed of a low shear micellar solution and a high-shear, highly aligned wormlike fluid state. While global rheological response is important in characterizing these wormlike micellar solutions, local velocity and concentration profiles provide a greater understanding of the phase separation/shear banding phenomena.

A variety of techniques, employed in previous studies, such as dynamic light scattering and NMR, have provided local velocity profiles of the shear-banded state. More recently, particle-tracking velocimetry [4] provided spatial and temporal information. However, there is little information provided about the microstructure of the high shear band due to optical turbidity. Therefore, SANS investigations under shear are of great value, especially a combination of studies in all three planes of the flow field, i.e., the flow-vorticity (radial beam configuration) velocity gradient-vorticity (tangential configuration), and the flow-velocity gradient (**1-2** plane) planes.

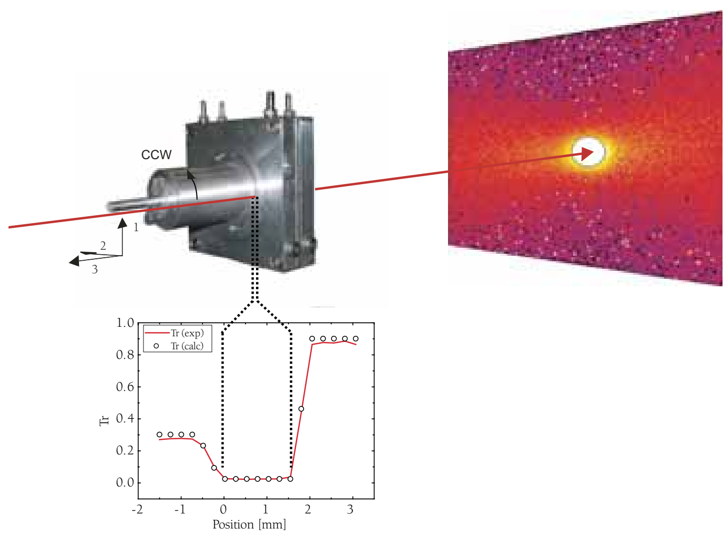

FIGURE 1: Illustration of the **1-2** plane shear cell in the neutron beam allowing for gap-resolved studies. The graph shows the recorded and predicted transmission as a function of beam position along the **2** axis using the 0.6 mm slit.

Small angle neutron scattering patterns collected in the **1-2** plane employed a newly designed aluminum Couette cell (15 mm inner radius, 2 mm gap and 10 mm path length) that is illustrated in Fig. 1. A slit preceding the cell reduced the neutron beam to 0.6 mm in width by 2.0 mm in height. The center of the narrowed beam could be positioned

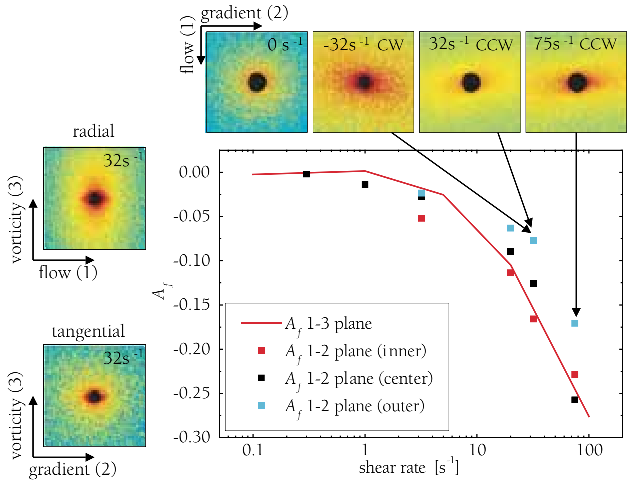

FIGURE 2: Scattering from 40mM EHAC and 300mM NaSal. Top: Scattering images from the **1-2** plane at shear rates 0, -32 s^{-1}, +32 s^{-1} and +75 s^{-1} from left to right. Left: Radial and tangential beam scattering images at 32 s^{-1}. Bottom right: Alignment factors of the radial and **1-2** plane experiments as a function of shear rate. Alignment A_f proceeds from zero at rest toward flow alignment at -1 with increasing shear rate. Beam position within the gap in the **1-2** plane is coded by color.

at 0.5 mm, 1 mm and 1.5 mm from the inner (rotating) wall. A stepper motor could attain shear rates from 0.1 s^{-1} to 100 s^{-1}, where positive shear rates correspond to rotation of the inner cylinder in a counterclockwise sense, looking through the cell toward the detector.

Figure 2 shows data recorded in all three planes of the flow field. The "radial" and "tangential" data were recorded in a conventional Couette cell with the rotation axis perpendicular to the beam. The radial scattering pattern displays a clear anisotropy along the vorticity axis while the tangential beam is isotropic. Hence the micelles are aligned parallel to the flow axis. The data from the **1-2** plane clearly demonstrate that micelles orient with a finite angle (between 0° and 45°) to the flow axis, and flow reversals demonstrate that this orientation changes sign, as expected. Note that data from the **1-2** plane are required to quantify both the degree and the angle of alignment. Indeed, the **1-2** plane SANS results are in quantitative agreement with independent flow birefringence measurements.

Segmental alignment factors A_f, are calculated from the scattering patterns, where $-1 < A_f < 0$ with 0 isotropic and -1 flow-aligned. As shown in Fig. 2, good agreement is observed for the alignment from both rheo-SANS devices, further validating the new **1-2** plane flow cell. However, the gap-resolved **1-2** plane data reveal important new information concerning the micellar structure in the shear banding state. Namely, there is increasing alignment closer to the rotating wall of the shear cell. This is expected as independent flow velocimetry measurements indicate that the shear rate is higher near the inner cylinder as a consequence of the flow kinematics and the shear thinning properties of the micelle solutions [5]. As nominal shear rates in the stress plateau region are probed, distinct bands form. The outer band has a shear rate of approximately 10 s^{-1} to 20 s^{-1}. An inner band exhibiting velocity fluctuations has shear rates higher than the nominal shear rates probed. At the start of the stress plateau, the enhanced degree of segmental alignment near the inner cylinder can be understood as a consequence of the higher local shear rate.

The true advantage of SANS over the other techniques is its ability to resolve microstructural information in the flowing, turbid region corresponding to SIPS. Sector averages oriented parallel and perpendicular to the nematic director are presented in Fig. 3 for two shear rates. At low shear rates no discernible differences in the intensity distributions at different gap positions are observed. At shear rates well into the shear-thinning region, however, the anisotropy and differences between both directions of the flow field and the different gap positions evolve. Most striking is the appearance of a q^{-4} decrease of the intensity at low q, referred to as Porod scattering. This behavior is usually attributed to scattering of a sharp interface and corresponds to fluctuations in scattering length density on length scales longer than the entanglement length of the wormlike micellar network, i.e., microphase separated domains are observed on these length scales in accordance with the observation of optical turbidity at high shear rates.

This study provides new evidence linking shear banding in wormlike micellar solutions to a shear-induced phase separation. Further analysis of these patterns is being undertaken to resolve the microstructure changes during SIPS.

Funding from Unilever and the Alexander von Humboldt Foundation is gratefully acknowledged.

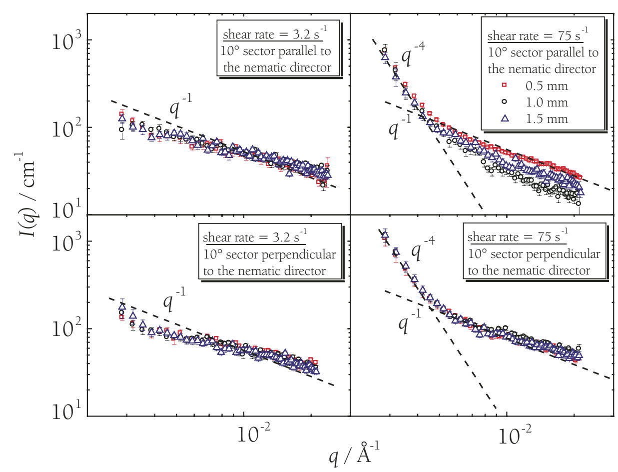

FIGURE 2: Radial intensity distributions in the zero shear plateau (left) and the shear-thinning regime (right) at three different gap positions along and perpendicular to the primary axis of micellar orientation. The q^{-4} regime corresponds to the onset of turbidity at high shear rates.

REFERENCES

[1] H. Rehage and H. Hoffmann, Mol. Phys. **74**, 933 (1991).

[2] M. E. Cates, J. Phys.-Condens. Mat. **8**, 9167 (1996).

[4] Y. T. Hu and A. Lips, J. Rheol., submitted.

[5] M. W. Liberatore, F. Nettesheim, L. Porcar and N. J. Wagner, Phys. Rev. Lett., submitted.